
EditRefiner: A Human-Aligned Agentic Framework for Image Editing Refinement

Zitong Xu¹, Huiyu Duan^{1†}, Yifei Nie³, Mingda Du³, Sijing Wu¹, Xionghuo Min¹, Tianyi Zheng², Jian Zhang², Shusong Xu², Jinwei Chen², Bo Li^{2†}, Guangtao Zhai^{1†}

¹Shanghai Jiao Tong University

²Vivo Mobile Communication Co., Ltd

³University of Electronic Science and Technology of China

[†]Corresponding Authors

Abstract

Recent text-guided image editing (TIE) models have made remarkable progress, yet edited images still frequently suffer from fine-grained issues such as unnatural objects, lighting mismatch, and unexpected changes. Existing refinement approaches either rely on costly iterative regeneration or employ vision-language models (VLMs) with weak spatial grounding, often resulting in semantic drift and unreliable local corrections. To address these limitations, we first construct **EditFHF-15K**, a dataset of fine-grained human feedback for edited images, comprising (1) 15K images from 12 TIE models spanning 43 editing tasks, (2) 60K annotated artifact regions and 80K editing failure regions, each accompanied by textual reasoning, and (3) 45K mean opinion scores (MOSs) assessing perceptual quality, instruction following, and visual consistency. Based on EditFHF-15K, we propose **EditRefiner**, a hierarchical, interpretable, and human-aligned agentic framework that reformulates post-editing correction as a human-like perception-reasoning-action-evaluation loop. Specifically, we introduce: (1) a perception agent that detects contextual saliency maps of artifacts and editing failures, (2) a reasoning agent that interprets these perceptual cues to perform human-aligned diagnostic inference, (3) an action agent that uses the reasoning output to plan and execute localized re-editing, and (4) an evaluation agent that assesses the re-edited image and guides the action agent on whether further refinements are required. Extensive experiments demonstrate that EditRefiner consistently outperforms state-of-the-art methods in distortion localization, diagnose accuracy and human perception alignment, establishing a new paradigm for self-corrective and perceptually reliable image editing. The code is available at <https://github.com/IntMeGroup/EditRefiner>.

1 Introduction

The rapid advancement of text-guided image editing (TIE) allows flexible image modifications through natural language instructions [8, 42, 35, 52, 2, 69]. Although some state-of-the-art editing models, such as Nano-Banana [8], Seedream4.0 [42], Qwen-Image-Edit [52], *etc.*, have achieved impressive performance, many edited images still suffer from subtle issues such as stiff limbs, lighting mismatch, unreadable text, and unintended changes. These flaws typically appear in localized areas of overall high-quality outputs, making them difficult to detect and costly to correct through full-image re-editing. Consequently, current TIE systems still lack an autonomous, fine-grained refinement framework, which remains a major barrier to real-world creative and industrial applications.

Recent research has explored three main strategies to improve the quality of TIE, including model fine-tuning [2, 69, 20], text prompt enhancement [48], and reinforcement learning-based optimization [33, 55, 60]. However, fine-tuning methods require large-scale, labor-intensive datasets; prompt enhancement approaches may introduce irrelevant or spurious information; and reinforcement learn-

ing techniques incur substantial computational cost. Moreover, although these approaches can improve overall realism, they lack explicit spatial reasoning and cannot reliably identify or correct local editing failures. With the emergence of vision-language models (VLMs) possessing advanced semantic reasoning, some works have explored using agentic framework to guide image generation [27, 44, 63]. However, accurately assessing image editing is inherently more complex than generation alone, as it requires VLMs to compare the edited image with the source and interpret the editing instructions. Moreover, strong knowledge priors of VLMs can override visual evidence, causing hallucinated judgments, highlighting the need to align TIE refinement agent with human perception.

In this work, we introduce **EditFHF-15K**, a dataset with fine-grained human feedback on edited images, curated by trained annotators following a rigorous and standardized annotation protocol. EditFHF-15K contains *15K* source images paired with edited images and their corresponding editing prompts, covering *43 editing tasks* and *13 state-of-the-art TIE models*. Based on the images, we further collect annotated *60K artifact regions* and *80K editing failure regions* for human-aligned perception agent development, with each region labeled using both semantic-level bounding boxes and pixel-level saliency maps. Each region is also accompanied by a human-annotated textual explanation to enable human-aligned reasoning agent construction. In addition, we collect *45K MOSs* on perceptual quality, instruction following, and visual consistency for human-aligned evaluation agent establishment. Building upon EditFHF-15K, we propose **EditRefiner**, a hierarchical, interpretable, and human-aligned agentic framework that reformulates post-editing correction as a structured **perception-reasoning-action-evaluation loop**. Through iterative verification, EditRefiner fuses perceptual cues, semantic reasoning, controllable re-editing, and human-aligned evaluation into a coherent self-corrective process, enabling automatic correction of fine-grained flaws in image editing. We conduct experiments on EditFHF-15K and other public TIE benchmarks, refining edited images generated by state-of-the-art editing models. The consistent performance gains across extensive datasets validate the effectiveness and robustness of EditRefiner.

The main contributions of this work include:

- We introduce EditFHF-15K, a dataset of fine-grained human feedback on edited images, comprising annotations of distortion regions, textual rationales, and preference ratings.
- We propose EditRefiner, a novel paradigm that reformulates post-editing as a perception-reasoning-action-evaluation loop, enabling automatic diagnosis and refinement for flaws.
- We design a collaborative four-agent system, where a perception agent performs context-aware flaw localization, a reasoning agent conducts human-aligned fine-grained diagnosis, an action agent executes controllable re-editing, and an evaluation agent assesses the refined results and guides further corrections.
- Extensive experiments on EditFHF-15K and other benchmarks demonstrate that EditRefiner consistently and effectively improves the quality of edited images, while performing regional cue extraction, semantic reasoning, and evaluation in better alignment with human preferences.

2 Related work

2.1 Text-guided image editing

Text-guided image editing has witnessed remarkable progress with the advent of large-scale diffusion models such as Stable Diffusion [41] and FLUX [12]. Early methods typically transform source image based on a target prompt, leveraging techniques such as attention control [5, 37] and noise inversion [22, 34, 23]. Subsequent works adopt fine-tuning method [2, 69, 20], which allows models to modify style or semantic content directly from an instruction prompt. More recently, unified models [52, 53, 59, 8, 42, 51] integrate understanding and generation within a single architecture, enabling flexible interpretation of editing instructions and producing highly realistic image edits. However, issues such as local artifacts, unnatural poses, and inconsistent lighting still occur [61, 60].

2.2 Visual quality assessment

Visual quality assessment (VQA) aims to evaluate visual content in alignment with human perception [11, 61, 62, 46, 45]. In the context of AIGC content assessment, most existing approaches [61, 46, 60] rely on global quantitative metrics, lacking explicit localization and fine-grained evaluation of local defects. To address this limitation, recently works [66, 27, 44] introduce predictors for

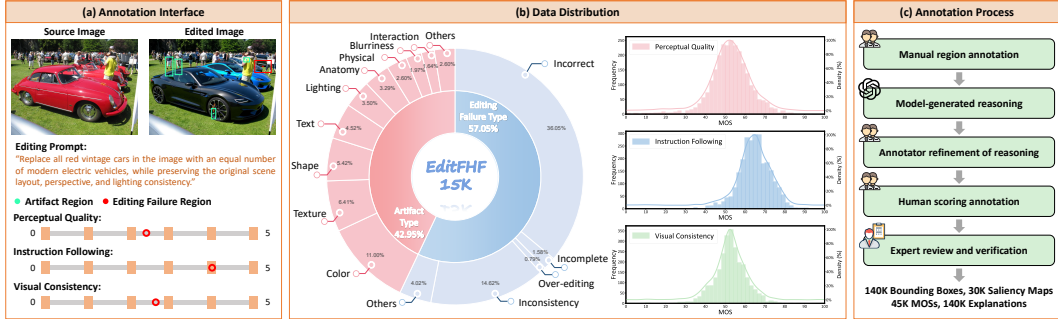


Figure 1: Overview of our EditFHF-15K. (a) An illustration of our annotation interface, (b) the distribution of flaw types and MOSs, (c) the human-AI collaborative annotation pipeline

local structural distortions. However, these methods are not designed for the image editing scenario, where evaluation must jointly consider the source image and the editing instruction.

2.3 Multi-agent system

Multi-agent systems have emerged with the advancement of VLMs for complex multimodal tasks [18, 26, 56, 7]. By enabling role specialization, collaboration, and iterative feedback, multi-agent frameworks can effectively decompose tasks, coordinate across agents, and progressively refine outputs [72, 25, 63, 29]. Such collaborative structures are particularly well-suited for scenarios requiring not only generation but also reasoning, assessing, and refining [63, 67]. In image generation applications, these capabilities are crucial for achieving high-quality results [44]. However, human-aligned agent frameworks for image editing remain unexplored.

3 EditFHF-15K

In this section, we introduce **EditFHF-15K**, a dataset of fine-grained human feedback on edited images. It comprises 15,287 edited images, each annotated with two saliency maps (artifact and editing failure) and three fine-grained scores (perceptual quality, instruction following, and visual consistency). The dataset also provides 60,318 bounding boxes for artifact regions and 80,345 bounding boxes for editing failure regions, with each box accompanied by a corresponding text describing the artifact or editing failure. This dataset facilitates the development of human-aligned systems capable of perception, reasoning, and evaluation of image editing.

3.1 Image collection

Considering practical relevance and real-world usage, we select 43 image editing tasks covering diverse operations. We collect 18K source images with editing prompts, including 10K sampled from Pico-Banana-400K [40] and EBench-18K [61], while the remaining 8K are gathered from publicly available photography websites, each accompanied by a textual description. Based on the image content and predefined editing tasks, we leverage the advanced VLM InternVL3.5 [49] to generate corresponding editing prompts, followed by careful manual verification and revision.

We then select 13 advanced TIE models, including both open-source and closed-source methods with diverse backbone architectures, to generate edited images with varied characteristics. We then use LMM4Edit [61] to score the results and retain the top three images for each editing instance, filtering out low-quality outputs while ensuring instruction consistency. More details are provided in Section ?? of the supplementary material.

3.2 Human annotation

To annotate the edited images, we first establish a rigorous annotation protocol. All annotators are required to undergo training and pass a qualification test. Only those who pass are allowed to participate in the annotation process. The overall annotation pipeline consists of three stages: regional annotation, textual annotation and scoring annotation.

3.2.1 Regional annotation

In the first stage, annotators are asked to identify artifact regions and editing failure regions, and annotate them using bounding boxes and disks. Specifically, bounding boxes are used to enclose the entire semantic object exhibiting a flaw, while disks with a radius of 1/20 of the image height are used to mark localized flawed areas. Each problematic semantic object is assigned one bounding box, and each bounding box must be associated with at least one disk.

The two types of regions are defined as follows: **(1) Artifact Region**: areas in the edited image that exhibit visual artifacts, such as unnatural textures, color inconsistencies, noise, or distortions. **(2) Editing Failure Region**: areas where the editing does not follow the instruction, including missing, incorrect, or unintended edits.

Each image is independently annotated by three annotators, who label the two region types separately. The results are then reviewed by an expert team. Finally, all disks are aggregated using Gaussian kernels to generate a pixel-level saliency map for each image. This stage produces both semantic-level bounding boxes and pixel-level saliency maps.

3.2.2 Textual annotation

In the second stage, we first employ the advanced VLM ChatGPT-5 [39] to generate initial descriptions for each flaw region. The model takes the source image, edited image, editing instruction, and bounding boxes as input. The bounding boxes serve as visual guidance, enabling more accurate and localized descriptions. Each prediction consists of a textual description that specifies the flaw type along with a corresponding reasoning statement, which explains the characteristics and visual details of the flaw within the associated region. These descriptions are then reviewed by three annotators in a round-robin manner, who may revise or rewrite them as needed. A description is finalized only when all three annotators reach agreement on its accuracy and completeness.

3.2.3 Scoring annotation

In the third stage, annotators are asked to rate each edited image across three evaluation dimensions: **(1) Perceptual Quality**: measures the overall visual quality of the edited image, including realism, absence of artifacts, structural integrity, color consistency, and richness of details. **(2) Instruction Following**: evaluates how well the edited image follows the given instruction, assessing whether the intended modifications are accurately and completely applied. **(3) Visual Consistency**: assesses how well the edited image maintains essential attributes of the source image beyond the intended edits, such as subject identity, key visual characteristics, and contextual consistency.

Each image is rated on a continuous 5-point scale by 15 annotators. During evaluation, annotators are provided with the source image, edited image, editing instruction, and the regional and textual annotations from previous stages, as shown in Figure 1(a). These annotations serve as references for scoring and are also implicitly validated during this process. Annotators can flag unreasonable annotations and any annotation identified as problematic by more than three annotators is discarded.

Following [21], ratings that deviate by more than two standard deviations from the mean are treated as outliers and removed. Annotators with more than 5% outlier ratings are excluded. The remaining scores are normalized into Z-scores and linearly scaled to the range [0, 100]. The final score for each image is computed as:

$$z_{ij} = \frac{s_{ij} - \mu_i}{\sigma_i}, \quad z_j = \frac{1}{N_j} \sum_{i=1}^{N_j} z_{ij}, \quad \text{Score}_j = \frac{100(z_j + 3)}{6} \quad (1)$$

where s_{ij} denotes the raw score assigned by the i -th annotator to the j -th image, μ_i and σ_i are the mean and standard deviation of annotator i , and N_j is the number of valid ratings for image j . This process yields reliable MOSs for each image across the three dimensions.

3.3 Data analysis

Through the three-stage annotation process, EditFHF-15K comprises 15,287 images, each associated with two saliency maps for artifact and editing failure. It contains 60,318 annotated artifact regions and 80,345 editing failure regions. Each annotated region is paired with a description averaging 32.6 words. Totally 687K human ratings are collected, which are aggregated to compute

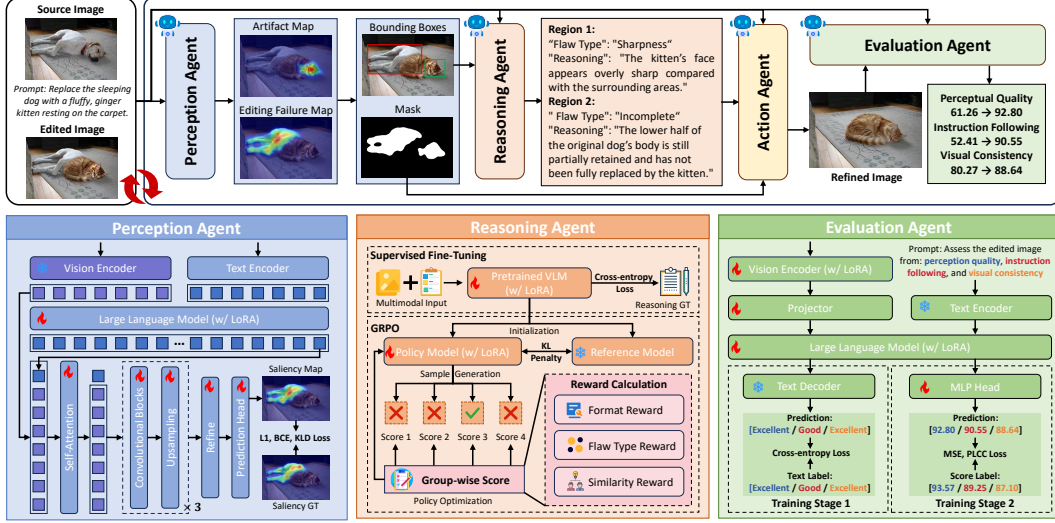


Figure 2: Overview of our EditRefiner. The framework operates as a perception-reasoning-action-evaluation loop for human-aligned post-editing correction.

45,861 MOS values across three dimensions: perceptual quality, instruction following, and visual consistency. The distribution of flaw types and MOSs are shown in Figure 1(b). More details of annotation pipeline are provided in Section ?? of supplementary material.

4 EditRefiner

4.1 Overall framework

EditRefiner is a multi-agent framework for human-aligned post-editing refinement. Unlike feed-forward editing pipelines with static corrections, it operates in a closed perception-reasoning-action-evaluation loop to autonomously identify and correct flaws. By integrating perceptual cues, semantic reasoning, and evaluation, EditRefiner produces refinements better aligned with human preferences.

As illustrated in Figure 2, the framework comprises **four collaborative agents**:

- **Perception Agent**: detects contextual saliency maps that highlight artifacts and editing failures in the image, providing a perceptual basis for subsequent analysis and refinement.
- **Reasoning Agent**: interprets perceptual cues and performs structured, human-aligned diagnostic inference to identify the flaw types and give the explanations.
- **Action Agent**: leverages the perception and reasoning outputs to plan and execute precise, localized re-editing operations.
- **Evaluation Agent**: evaluates the re-edited image against three dimensions, providing feedback that informs whether additional refinements are required.

Formally, let I_t denote the edited image at iteration t , I_0 the source image, and T the editing instruction. The *Perception Agent* generates two saliency maps, S_A highlighting artifacts and S_F highlighting editing failure. Each map S_i is thresholded to produce a corresponding mask $M_{i,t}$ and bounding boxes $B_{i,t}$ for the flawed regions.

$$M_{i,t}, B_{i,t} = \text{PerceptionAgent}(\{I_0, T\}, I_t) \quad (2)$$

Based on the bounding boxes $B_{i,t}$, the *Reasoning Agent* produces an overall description $D_{i,t}$ containing flaw types and explanations.

$$D_{i,t} = \text{ReasoningAgent}(\{I_0, T\}, I_t, B_{i,t}) \quad (3)$$

The *Action Agent* then applies localized corrections based on description $D_{i,t}$ and mask $M_{i,t}$ to obtain the updated image, where the task-specific descriptions and masks, corresponding to either artifacts or editing failures, are aggregated into unified representations D_t and M_t , respectively.

$$I_{t+1} = \text{ActionAgent}(\{I_0, T\}, I_t, \{M_t, D_t\}), \quad t \leftarrow t + 1 \quad (4)$$

After each re-editing step, an Evaluation Agent assesses the updated image in terms of perceptual quality (s_v), instruction adherence (s_e), and visual consistency (s_p), and computes the overall score ($s_{overall}$), following [61].

$$s_v, s_e, s_p = \text{EvaluationAgent}(\{I_0, T\}, I_{t+1}), \quad s_{overall} = s_v^{0.3} * s_e^{0.4} * s_p^{0.3} \quad (5)$$

The refinement loop is terminated when there is no improvement in the overall score, or when the maximum number of editing iterations is reached. This threshold-based stopping criterion effectively prevents unnecessary refinement and avoids cascading degradation. By integrating perception, reasoning, action, and evaluation, the framework enables step-wise, interpretable, and perceptually faithful refinement with controllable iterative corrections.

4.2 Perception Agent

To mimic human perceptual sensitivity, we develop a perception agent to estimate a saliency map $S \in [0, 1]^{H \times W}$, conditioned on both source image I_0 , edited image I_e and editing prompt T . This task requires jointly understanding the instruction prompt, visual content, and comparing the source and edited images, making VLMs a natural choice due to their strong multimodal fusion and visual understanding capabilities. We adopt a VLM as the backbone and attach a saliency decoder for pixel-level prediction. To address the limitation of early fusion, we concatenate the vision encoder features with the final-layer hidden states. The fused features are then fed into the saliency decoder to produce the saliency map. The model is optimized with a hybrid saliency loss L_{sal} :

$$L_{sal} = \alpha L_{L1}(S, \hat{S}) + \beta L_{BCE}(S, \hat{S}) + (1 - \alpha - \beta) L_{KLD}(S, \hat{S}), \quad (6)$$

where \hat{S} is the ground-truth saliency map. The L1 loss L_{L1} enforces pixel-level accuracy, the binary cross-entropy loss L_{BCE} encourages the model to distinguish flawed from non-flawed regions, and the KL divergence loss L_{KLD} aligns the predicted saliency map with human perceptual distributions.

The predicted saliency map is thresholded with τ to produce a binary mask M and bounding boxes B . The bounding boxes B serve as spatial priors, providing perceptual cues to guide the analysis of Reasoning Agent, while mask M directly highlights flawed regions for Action Agent to perform localized correction.

4.3 Reasoning Agent

Given the bounding boxes $\{B\}$, the Reasoning Agent performs structured diagnosis, generating textual descriptions $\{D\}$ that include flaw types and reasoning statements. This requires human-aligned reasoning rather than simple classification or captioning.

We adopt a two-stage preference alignment paradigm to train a VLM. In the first stage, **Supervised Fine-Tuning (SFT)**, the reasoning model is initialized with structured response formats, and trained using cross-entropy loss.

In the second stage, **Group Relative Policy Optimization (GRPO)**, the model aligns its reasoning behavior with human preferences through reinforcement signals:

$$L_{GRPO} = \mathbb{E} \left[\min(r_t \hat{A}_t, \text{clip}(r_t, 1 - \epsilon, 1 + \epsilon) \hat{A}_t) - \beta D_{KL}[\pi_\theta || \pi_{ref}] \right], \quad (7)$$

where \hat{A}_t captures normalized advantages computed from the reward function, which consists of format reward, flaw type reward, and similarity reward, with details provided in the supplementary. This stage ensures consistent, human-aligned reasoning across diverse flaws.

4.4 Action Agent

Building on the reasoning outputs, the Action Agent translates the diagnostic information D into a controllable re-editing instruction that specifies how the image should be corrected. It then provides the source image, the edited image from the previous iteration, the generated editing instruction, and the mask M highlighting the regions requiring modification as input to an editing model. The model, which supports multiple image editing operations, produces a re-edited image that progressively corrects flaws and better aligns with the desired output.

4.5 Evaluation Agent

The Evaluation Agent assesses the quality of re-edited images along three human-aligned dimensions: perceptual quality, instruction following, and visual consistency. It is built upon a VLM and

Table 1: Performance of **EditRefiner** on EditFHF-15K, GEdit-Bench [30], I2I-Bench [47], and KRIS-Bench [58]. **PQ**: Perceptual Quality, **IF**: Instruction Following, **VC**: Visual Consistency, **PP**: Physical Plausibility. Better performances over baseline are **bolded**.

Benchmark Method/Dimensions	EditFHF-15K				GEdit-Bench [30]			I2IBench [47]					KRIS-Bench [57]			
	PQ	IF	VC	Average	PQ	IF	Average	PQ	IF	VC	PP	Average	PQ	IF	VC	Average
Qwen-Image-Edit [52]	69.38	63.15	67.33	66.62	7.872	8.011	7.941	0.811	0.931	0.898	0.527	0.792	80.25	61.37	70.28	70.63
(w/Reasoning Agent)	72.06	65.53	66.24	67.94	7.946	7.961	7.954	0.815	0.933	0.879	0.543	0.792	79.06	63.53	70.24	70.94
$\Delta\%(\uparrow)$	+3.86	+3.77	-1.62	+1.99	+0.94	-0.62	+0.15	+0.41	+0.15	-2.11	+2.98	+0.05	-1.48	+3.52	-0.06	+0.44
(w/EditRefiner)	74.20	71.50	72.05	72.58	8.182	8.431	8.306	0.836	0.945	0.920	0.565	0.816	82.06	68.53	72.31	74.30
$\Delta\%(\uparrow)$	+6.95	+13.2	+7.01	+8.95	+3.94	+5.24	+4.60	+3.06	+1.49	+2.39	+7.21	+3.10	+2.26	+11.67	+2.89	+5.19
NanoBanana [8]	70.51	65.86	69.21	68.53	7.810	8.212	8.011	0.805	0.933	0.903	0.542	0.796	81.74	63.21	71.90	72.28
(w/Reasoning Agent)	70.96	68.28	71.55	70.26	7.894	8.285	8.089	0.803	0.938	0.904	0.557	0.800	82.63	64.08	72.01	72.91
$\Delta\%(\uparrow)$	+0.64	+3.68	+3.38	+2.57	+1.08	+0.89	+0.98	-0.31	+0.53	+0.19	+2.71	+0.59	+1.09	+1.38	+0.15	+0.87
(w/EditRefiner)	75.20	70.45	73.82	73.16	8.216	8.644	8.430	0.830	0.938	0.922	0.572	0.816	84.17	68.27	75.82	76.09
$\Delta\%(\uparrow)$	+6.65	+6.97	+6.66	+6.76	+5.20	+5.26	+5.23	+3.03	+0.58	+2.21	+5.48	+2.50	+2.97	+8.00	+5.45	+5.48
Seedream4.0 [42]	68.27	66.18	65.24	66.56	7.650	7.941	7.795	0.815	0.917	0.891	0.519	0.786	82.56	62.49	69.88	71.64
(w/Reasoning Agent)	70.04	65.12	65.15	66.77	7.722	7.965	7.843	0.822	0.920	0.883	0.526	0.788	82.04	64.12	70.25	72.14
$\Delta\%(\uparrow)$	+2.59	-1.60	-0.14	0.32	+0.94	+0.30	+0.62	+0.87	+0.32	-0.95	+1.39	+0.28	-0.63	+2.61	+0.53	+0.84
(w/EditRefiner)	71.46	70.28	70.84	70.86	7.981	8.244	8.113	0.838	0.937	0.906	0.539	0.805	85.28	66.15	73.04	74.82
$\Delta\%(\uparrow)$	+4.67	+6.20	+8.58	+6.48	+4.33	+3.82	+4.07	+2.80	+2.19	+1.68	+3.74	+2.46	+3.30	+5.86	+4.52	+4.56



Figure 3: Example results from advanced TIE models and results with our EditRefiner. Additional results are provided in the supplementary material.

a trainable MLP scoring head. The VLM extracts rich visual and semantic representations, which are then processed by the scoring head to predict quantitative scores. The model is trained in two stage. In the first stage, continuous scores are converted into five textual levels (bad, poor, fair, good, excellent) and optimized with cross-entropy loss. In the second stage, the model is trained using a combination of mean squared error (MSE) loss and Pearson linear correlation coefficient (PLCC) loss across all three dimensions. The losses are computed as

$$L_{\text{score}} = \sum_d \left(L_{\text{MSE}}^{(d)} + L_{\text{PLCC}}^{(d)} \right), \quad (8)$$

where $d \in \{\text{perceptual quality, instruction following, visual consistency}\}$. This total loss ensures that the predicted scores are both accurate and well-correlated with human judgments across all three evaluation dimensions. The Evaluation Agent provides human-aligned scores to guide the loop, ensuring high-quality re-edited images and enabling appropriate termination.

The proposed multi-agent framework integrates perception-driven diagnosis, context-aware reasoning, controllable re-editing, and multi-dimensional assessing within a unified loop, enabling interpretable and autonomous refinement in better alignment with human preferences.

5 Experiments

5.1 Experimental setup

Training Configuration. We train the EditRefiner on our EditFHF-15K, which is split to training, validating and testing set with a 4:1:1 ratio. The Perception, Reasoning, and Evaluation Agents are

Table 2: Quantitative evaluation and ablation of the Perception Agent on flaw-aware saliency prediction. ♠ hand-crafted methods, ♡ deep learning-based methods, ★ general-purpose VLMs. The fine-tuned results are marked with *. The best results are highlighted in red, and the second-best results are highlighted in blue.

Dimension Method/Metric	Artifact Region					Editing Failure Region				
	AUC-Judd ↑	NSS↑	CC ↑	SIM↑	KLD↓	AUC-Judd ↑	NSS↑	CC ↑	SIM↑	KLD↓
♠AIM [3]	0.7223	1.1476	0.1689	0.0794	3.0217	0.6395	0.5283	0.1427	0.0416	7.3412
♠SMVJ [6]	0.7169	0.7093	0.0786	0.0631	3.3698	0.5821	0.3538	0.0714	0.0426	7.5923
♠SWD [71]	0.7176	0.5294	0.0708	0.0757	3.5219	0.5912	0.3876	0.0941	0.0493	6.8115
♠CA [14]	0.5528	0.4619	0.1016	0.0687	3.3325	0.5234	0.0941	0.0548	0.0615	7.6489
♡ResNet-50 [16]*	0.7816	1.4498	0.4674	0.1768	3.0173	0.6882	0.8536	0.1492	0.0731	4.1964
♡SALICON [19]*	0.8227	1.5791	0.5028	0.2721	2.7194	0.7093	0.9845	0.4586	0.2487	3.5635
♡MLNet [9]*	0.7536	1.5462	0.3527	0.2394	2.2371	0.7235	0.9588	0.3186	0.2243	3.4927
♡SAM-ResNet [10]*	0.8357	1.8574	0.4031	0.4469	2.0716	0.7416	0.9821	0.3724	0.3015	2.8478
♡TranSalNet [31]*	0.8034	1.7481	0.4598	0.4013	2.8692	0.7438	1.4426	0.4187	0.3045	3.1076
♡RichHF [27]*	0.8508	1.7976	0.4739	0.4298	2.6721	0.7523	1.6247	0.4315	0.3326	2.8914
★Ovis2.5-9B [32]	0.6137	0.4184	0.1693	0.2472	7.4321	0.6598	0.6845	0.1487	0.2319	6.8123
★InternVL3.5-8B [49]	0.6046	0.7713	0.2096	0.3087	6.9341	0.6732	0.9024	0.1683	0.2896	5.1875
★Qwen3-VL-8B [65]	0.6121	0.4215	0.1704	0.2496	6.4387	0.6814	1.0926	0.1511	0.3042	4.8956
★ChatGPT-5 [38]	0.7463	0.7217	0.2612	0.2913	6.0064	0.7138	1.2034	0.2526	0.3035	3.5872
★Gemini-3.1-Pro [15]	0.7071	0.7198	0.2597	0.2896	6.0142	0.7316	1.3115	0.3013	0.3224	3.3619
Ours (Ovis2.5-9B)*	0.8035	1.5086	0.4184	0.3795	2.2042	0.7794	1.5267	0.3421	0.3618	2.9937
Ours (InternVL3.5-8B)*	0.8431	1.8476	0.4792	0.4687	2.2073	0.8015	1.6014	0.4528	0.4212	2.3968
Ours (Qwen3-VL-8B)*	0.8720	2.0256	0.5550	0.4901	1.9515	0.8306	1.8925	0.5142	0.4578	2.2191

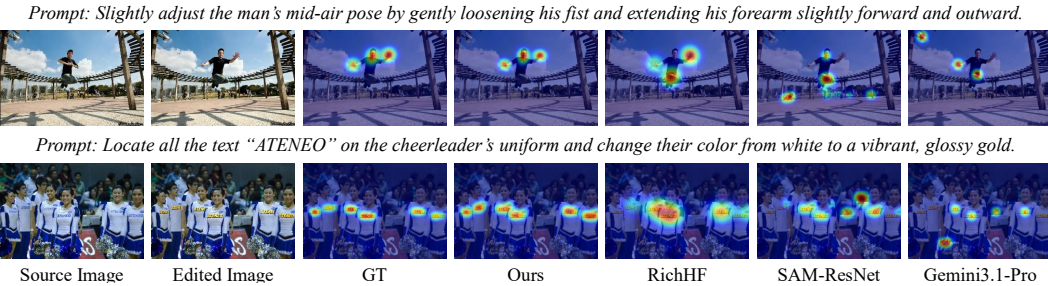


Figure 4: Visualization of saliency map prediction. Our method produces sharper and more precise localization. The first row highlights artifact regions, while the second row shows editing failure regions.

fine-tuned via LoRA [17] based on the Qwen3-VL-8B [65] backbone. Inference is fully automatic, converging in an average of 2.53 iterations with a maximum of 4.

Evaluation Datasets and Metrics. To evaluate the refinement capability and validate generalization, we report results on EditFHF-15K, GEdit-Bench [30], I2I-Bench [47], and KRIS-Bench [58]. Results are averaged over five runs with different random seeds for stability. We use the Evaluation Agent of EditRefiner as the evaluation metric on EditFHF-15K, while following the respective evaluation protocols for the other benchmarks. For individual modules, following [4, 44], Perceptual Agent is evaluated using CC, SIM, KLD, AUC-Judd, and NSS. Reasoning Agent is assessed via distortion classification accuracy and semantic alignment with ROUGE [28], METEOR [1], Word2Vec [36], and SimCSE [13]. Evaluation Agent is measured using SRCC, KRCC, and PLCC.

5.2 Comparison results

5.2.1 Overall system performance

As shown in Table 1, the performance of EditRefiner across various benchmarks demonstrates its strong capability in enhancing image editing. The Reasoning Agent alone can provide performance gains, but its effectiveness is limited due to the lack of explicit local region information. In contrast, EditRefiner consistently achieves substantial improvements across different evaluation settings. Figure 3 further presents qualitative comparisons across various scenes and prompt conditions.

5.2.2 Individual agent analysis

Perception Agent. Table 2 compares our Perception Agent with conventional saliency detectors, learning-based methods, and general-purpose VLMs. Hand-crafted methods rely on low-level cues and fail to capture semantics, while learning-based approaches lack editing-specific understanding, leading to inaccurate localization. General-purpose VLMs also perform poorly due to insufficient task grounding. In contrast, our method achieves state-of-the-art performance across all metrics.

Table 3: Quantitative evaluation and ablation of the Reasoning Agent. The best results are **bolded**.

Dimension Method/Metric	Artifact Region					Editing Failure Region				
	Accuracy ↑	SimCSE↑	Word2Vec↑	Meteor ↑	ROUGE ↑	Accuracy ↑	SimCSE↑	Word2Vec↑	Meteor ↑	ROUGE ↑
ChatGPT-5 [38]	62.18%	0.6728	0.5846	0.1550	0.1304	68.25%	0.6532	0.5429	0.1526	0.1280
Gemini-3.1-Pro [15]	60.91%	0.6883	0.6281	0.1689	0.1137	66.48%	0.6637	0.5824	0.1671	0.1112
Ovis2.5-9B [32]	58.12%	0.6694	0.6136	0.1665	0.0746	63.27%	0.6468	0.5681	0.1642	0.0729
Ovis2.5-9B + GRPO	64.36%	0.7057	0.6628	0.2226	0.1518	69.01%	0.6812	0.6153	0.1704	0.1295
Ovis2.5-9B + SFT	72.96%	0.8012	0.7495	0.3586	0.3389	80.11%	0.8036	0.7132	0.3508	0.3165
Ours (GRPO + SFT)	80.67%	0.8461	0.7819	0.4052	0.3554	82.93%	0.8264	0.7376	0.3967	0.3428
InternVL3.5-8B [49]	58.73%	0.6759	0.6214	0.1687	0.0979	64.05%	0.6526	0.5741	0.1659	0.0956
InternVL3.5-8B + GRPO	60.82%	0.7216	0.6278	0.1815	0.1243	66.14%	0.6968	0.5856	0.1782	0.1217
InternVL3.5-8B + SFT	77.88%	0.8389	0.7762	0.3948	0.3561	79.22%	0.8197	0.7318	0.3875	0.3439
Ours (GRPO + SFT)	79.94%	0.8443	0.7846	0.4206	0.3789	81.02%	0.8258	0.7397	0.4093	0.3642
Qwen3-VL-8B [65]	57.38%	0.6835	0.6082	0.1661	0.1049	62.77%	0.6613	0.5667	0.1634	0.1023
Qwen3-VL-8B + GRPO	70.14%	0.7498	0.7084	0.2183	0.2482	72.63%	0.7451	0.6529	0.2451	0.2036
Qwen3-VL-8B + SFT	79.31%	0.8324	0.7649	0.3567	0.3268	80.58%	0.8127	0.7196	0.3489	0.3149
Ours (GRPO + SFT)	81.08%	0.8527	0.7856	0.3942	0.3704	84.36%	0.8338	0.7421	0.3859	0.3485

Table 4: Quantitative evaluation of the Evaluation Agent. ♠ Hand-crafted VQA metrics, ♣ deep learning-based VQA methods, ★ general-purpose VLMs, ☆ editing-oriented VLMs. The fine-tuned results are marked with *. The best results are highlighted in **red**, and the second-best results are highlighted in **blue**.

Dimension Methods/Metrics	Perceptual Quality			Instruction Following			Visual Consistency			Overall Score		
	SRCC	KRCC	PLCC	SRCC	KRCC	PLCC	SRCC	KRCC	PLCC	SRCC	KRCC	PLCC
♣GMSD [64]	0.1274	0.0776	0.1853	0.1081	0.0723	0.1059	0.1068	0.1035	0.1534	0.1641	0.0988	0.1628
♠SSIM [50]	0.1004	0.0907	0.1199	0.1055	0.0698	0.1080	0.1165	0.0113	0.1103	0.1470	0.1023	0.1602
♠VIF [43]	0.2196	0.1786	0.2761	0.0959	0.0640	0.1035	0.2007	0.1657	0.2650	0.2121	0.1801	0.2326
♠LPIPS [70]	0.3435	0.1960	0.3032	0.1244	0.0823	0.3332	0.2457	0.1976	0.3083	0.3079	0.2486	0.3249
♣CVRKD* [68]	0.6507	0.4721	0.7244	0.1802	0.1209	0.1963	0.5371	0.3814	0.6208	0.4507	0.3221	0.4622
♠AHIQ* [24]	0.7172	0.5321	0.7779	0.2385	0.1612	0.2510	0.6583	0.4136	0.6775	0.4880	0.3209	0.5015
♣Q-Align* [54]	0.7565	0.6640	0.7650	0.5663	0.4120	0.5971	0.6856	0.4948	0.7123	0.6095	0.4230	0.6208
☆Ovis2.5-9B [32]	0.1010	0.1008	0.1726	0.1121	0.0886	0.1428	0.2209	0.1897	0.1345	0.2017	0.1661	0.2405
★Qwen3-VL-8B [65]	0.2455	0.2075	0.2236	0.2412	0.2327	0.2365	0.2772	0.2604	0.3292	0.2536	0.2315	0.2601
★InternVL3-8B [49]	0.2328	0.2079	0.2747	0.2059	0.1859	0.1649	0.3226	0.2796	0.3618	0.2531	0.2242	0.2621
★ChatGPT-5 [39]	0.3309	0.2631	0.3749	0.2786	0.2127	0.3133	0.3383	0.2343	0.4156	0.3559	0.2961	0.3680
☆Gemini-3.1-Pro [15]	0.3115	0.2874	0.3386	0.2927	0.2618	0.2966	0.3009	0.2396	0.3704	0.3410	0.2927	0.3651
☆LMM4Edit [61]	0.3509	0.2424	0.3651	0.3385	0.2109	0.3457	0.3555	0.2145	0.3552	0.3883	0.3006	0.3851
☆EditScore (Qwen3) [33]	0.2068	0.1515	0.1842	0.2632	0.2262	0.1316	0.2886	0.2451	0.1274	0.2829	0.2270	0.2497
☆EditReward (MiMo) [55]	0.3276	0.2519	0.3357	0.0508	0.0336	0.0683	0.2627	0.2087	0.2679	0.3037	0.2647	0.3251
☆EditHF [60]	0.2082	0.1427	0.1416	0.1325	0.0886	0.1191	0.1520	0.1023	0.1365	0.1412	0.1225	0.1323
Ours (Ovis2.5-9B)*	0.7233	0.5371	0.7471	0.7100	0.5281	0.7212	0.6797	0.4126	0.7295	0.7643	0.6626	0.7826
Ours (InternVL3.5-8B)*	0.7335	0.5044	0.7278	0.7244	0.5409	0.7353	0.6952	0.5088	0.7332	0.8177	0.7221	0.8346
Ours (Qwen3-VL-8B)*	0.7852	0.6686	0.8014	0.7522	0.6508	0.7641	0.7885	0.6412	0.7969	0.8723	0.7235	0.8842

Table 5: Ablation of turn number. The best results are **bolded**.

Benchmark Turns/Method	EditHF-15K			GEdit-Bench [30]			I2IBench [47]			KRIS-Bench [57]		
	Qwen [52]	Nano [8]	Seed [42]	Qwen [52]	Nano [8]	Seed [42]	Qwen [52]	Nano [8]	Seed [42]	Qwen [52]	Nano [8]	Seed [42]
Turn 0	66.62	68.53	66.56	7.941	8.011	7.795	0.792	0.796	0.786	70.63	72.28	71.64
Turn 1	69.28	71.02	68.91	8.192	8.244	8.036	0.807	0.809	0.800	72.74	74.51	73.33
Turn 2	71.11	71.36	69.84	8.167	8.298	8.052	0.805	0.808	0.801	72.98	74.83	73.58
Turn 3	72.52	72.94	70.40	8.233	8.421	8.101	0.809	0.811	0.803	73.26	75.21	73.92
Turn 4	72.64	73.05	70.72	8.311	8.438	8.097	0.814	0.814	0.801	74.34	76.08	74.89
Auto Stop	72.58	73.16	70.86	8.306	8.430	8.113	0.816	0.816	0.805	74.30	76.09	74.82

Figure 4 further shows that our saliency maps exhibit sharper spatial focus and better alignment with human annotations, providing a reliable basis for subsequent reasoning and refinement.

Reasoning Agent. Table 3 presents results under different training strategies. Across VLM backbones, our method consistently improves all metrics, showing that joint SFT and GRPO training enhances reasoning accuracy and better aligns with human preferences than either alone. After training on our dataset, the Reasoning Agent surpasses advanced closed-source models such as ChatGPT-5 and Gemini-3.1-Pro, demonstrating strong capability in identifying editing-related reasoning gaps and enabling human-aligned adaptation.

Evaluation Agent. Table 4 compares the Evaluation Agent with existing VQA methods. Hand-crafted methods perform poorly due to focus on low-level distortions, while deep learning-based approaches improve visual assessment but remain limited in evaluating editing alignment. General-purpose VLMs lack task-specific understanding, and editing-oriented VLMs still struggle with accurate scoring for high-quality results. In contrast, our Evaluation Agent achieves the best alignment with human preferences across all dimensions, providing reliable feedback for iterative refinement.

5.3 Ablation study

Table 2, 3, 4, show the performance of the agents across different VLM backbones, where consistent improvements are observed, validating the effectiveness of our training strategy and our dataset. We further conduct ablations on the number of refinement turns, as shown in Table 5, indicating significant improvements within the first 1-2 iterations, while performance gradually saturates at 3-4

turns. Notably, the 4th iteration does not consistently surpass our auto-stop strategy, as excessive re-editing not only increases computational cost but also leads to error accumulation and potential subject drift. Additional ablation studies are provided in Section ?? of the supplementary material.

6 Conclusion

In this paper, we introduce EditFHF-15K, a large-scale dataset of fine-grained human feedback that provides rich annotations of editing flaw regions, textual reasoning, and human ratings across diverse editing models and tasks. Built upon this dataset, we propose EditRefiner, a hierarchical and interpretable agentic framework that reformulates image refinement as a perception-reasoning-action-evaluation loop. Experiments show that EditRefiner outperforms state-of-the-art methods in flaw localization, reasoning, and human preference alignment, highlighting its potential for self-corrective, human-aligned image editing.

References

- [1] Banerjee, S., Lavie, A.: METEOR: An automatic metric for MT evaluation with improved correlation with human judgments. In: Proceedings of the ACL Workshop on Intrinsic and Extrinsic Evaluation Measures for Machine Translation and/or Summarization (ACL Workshop). pp. 65–72 (Jun 2005)
- [2] Brooks, T., Holynski, A., Efros, A.A.: Instructpix2pix: Learning to follow image editing instructions. In: Proceedings of the IEEE/CVF Conference on Computer Vision and Pattern Recognition (CVPR). pp. 18392–18402 (2023)
- [3] Bruce, N., Tsotsos, J.: Saliency based on information maximization. In: Weiss, Y., Schölkopf, B., Platt, J. (eds.) NIPS. vol. 18. MIT Press (2005), https://proceedings.neurips.cc/paper_files/paper/2005/file/0738069b244a1c43c83112b735140a16-Paper.pdf
- [4] Bylinskii, Z., Judd, T., Oliva, A., Torralba, A., Durand, F.: What do different evaluation metrics tell us about saliency models? IEEE transactions on pattern analysis and machine intelligence (TPAMI) **41**(3), 740–757 (2019)
- [5] Cao, M., Wang, X., Qi, Z., Shan, Y., Qie, X., Zheng, Y.: Masactrl: Tuning-free mutual self-attention control for consistent image synthesis and editing. In: Proceedings of the IEEE/CVF international conference on computer vision (CVPR). pp. 22560–22570 (2023)
- [6] Cerf, M., Harel, J., Einhaeuser, W., Koch, C.: Predicting human gaze using low-level saliency combined with face detection. In: Platt, J., Koller, D., Singer, Y., Roweis, S. (eds.) NIPS. vol. 20. Curran Associates, Inc. (2007), https://proceedings.neurips.cc/paper_files/paper/2007/file/708f3cf8100d5e71834b1db77dfa15d6-Paper.pdf
- [7] Chan, C.M., Chen, W., Su, Y., Yu, J., Xue, W., Zhang, S., et al.: Chateval: Towards better llm-based evaluators through multi-agent debate. In: Proceedings of the International Conference on Learning Representations (ICLR). pp. 1–9 (2023)
- [8] Comanici, G., Bieber, E., Schaekermann, M., Pasupat, I., Sachdeva, N., Dhillon, I., et al.: Gemini 2.5: Pushing the frontier with advanced reasoning, multimodality, long context, and next generation agentic capabilities. arXiv preprint arXiv:2507.06261 (2025)
- [9] Cornia, M., Baraldi, L., Serra, G., Cucchiara, R.: A Deep Multi-Level Network for Saliency Prediction. In: ICPR (2016)
- [10] Cornia, M., Baraldi, L., Serra, G., Cucchiara, R.: Predicting Human Eye Fixations via an LSTM-based Saliency Attentive Model. IEEE Transactions on Image Processing **27**(10), 5142–5154 (2018)
- [11] Duan, H., Hu, Q., Wang, J., Yang, L., Xu, Z., Liu, L., Min, X., Cai, C., Ye, T., Zhang, X., Zhai, G.: Finevq: Fine-grained user generated content video quality assessment. In: Proceedings of the IEEE/CVF Conference on Computer Vision and Pattern Recognition (CVPR) (2025)
- [12] Esser, P., Kulal, S., Blattmann, A., Entezari, R., Müller, J., Saini, H., et al.: Scaling rectified flow transformers for high-resolution image synthesis. In: Proceedings of the International Conference on Machine Learning (ICML) (2024)
- [13] Gao, T., Yao, X., Chen, D.: SimCSE: Simple contrastive learning of sentence embeddings. In: Proceedings of the Conference on Empirical Methods in Natural Language Processing (EMNLP) (2021)
- [14] Goferman, S., Zelnik-Manor, L., Tal, A.: Context-aware saliency detection. In: 2010 IEEE Computer Society Conference on Computer Vision and Pattern Recognition. pp. 2376–2383 (2010). <https://doi.org/10.1109/CVPR.2010.5539929>
- [15] Google DeepMind: Gemini 3.1 pro: Best for complex tasks and bringing creative concepts to life. <https://deepmind.google/models/gemini/pro/> (2025)
- [16] He, K., Zhang, X., Ren, S., Sun, J.: Deep residual learning for image recognition. In: Proceedings of the IEEE/CVF Conference on Computer Vision and Pattern Recognition (CVPR). pp. 770–778 (2016)

- [17] Hu, E.J., Shen, Y., Wallis, P., Allen-Zhu, Z., Li, Y., Wang, S., et al.: Lora: Low-rank adaptation of large language models. In: Proceedings of the International Conference on Learning Representations (ICLR) (2022)
- [18] Huang, X., Liu, W., Chen, X., Wang, X., Wang, H., Lian, D., Wang, Y., Tang, R., Chen, E.: Understanding the planning of llm agents: A survey. arXiv preprint arXiv:2402.02716 (2024)
- [19] Huang, X., Shen, C., Boix, X., Zhao, Q.: Salicon: Reducing the semantic gap in saliency prediction by adapting deep neural networks. In: ICCV (December 2015)
- [20] Hui, M., Yang, S., Zhao, B., Shi, Y., Wang, H., Wang, P., et al.: Hq-edit: A high-quality dataset for instruction-based image editing. arXiv preprint arXiv:2404.09990 (2024)
- [21] (ITU), I.T.U.: Methodology for the subjective assessment of the quality of television pictures. Tech. Rep. Rec. ITU-R BT.500-13, International Telecommunication Union (ITU) (Jan 2012)
- [22] Ju, X., Zeng, A., Bian, Y., Liu, S., Xu, Q.: Pnp inversion: Boosting diffusion-based editing with 3 lines of code. In: Proceedings of the International Conference on Learning Representations (ICLR) (2024)
- [23] Kulikov, V., Kleiner, M., Huberman-Spiegelglas, I., Michaeli, T.: Flowedit: Inversion-free text-based editing using pre-trained flow models. In: Proceedings of the IEEE/CVF International Conference on Computer Vision (ICCV). pp. 19721–19730 (2025)
- [24] Lao, S., Gong, Y., Shi, S., Yang, S., Wu, T., Wang, J., et al.: Attentions help cnns see better: Attention-based hybrid image quality assessment network. In: Proceedings of the IEEE/CVF Conference on Computer Vision and Pattern Recognition (CVPR) Workshops. pp. 1140–1149 (2022)
- [25] Li, H., Zhang, M., Zheng, D., Guo, Z., Jia, Y., Feng, K., et al.: Editthinker: Unlocking iterative reasoning for any image editor. arXiv preprint arXiv:2512.05965 (2025)
- [26] Liang, T., He, Z., Jiao, W., Wang, X., Wang, Y., Wang, R., et al.: Encouraging divergent thinking in large language models through multi-agent debate. arXiv preprint arXiv:2305.19118 (2023)
- [27] Liang, Y., He, J., Li, G., Li, P., Klimovskiy, A., Carolan, N., Sun, J., Pont-Tuset, J., Young, S., Yang, F., et al.: Rich human feedback for text-to-image generation. In: Proceedings of the IEEE/CVF Conference on Computer Vision and Pattern Recognition (CVPR). pp. 19401–19411 (2024)
- [28] Lin, C.Y.: ROUGE: A package for automatic evaluation of summaries. In: Text Summarization Branches Out. pp. 74–81. Association for Computational Linguistics, Barcelona, Spain (Jul 2004), <https://aclanthology.org/W04-1013/>
- [29] Liu, L., Cai, C., Shen, S., Liang, J., Ouyang, W., Ye, T., Mao, J., Duan, H., Yao, J., Zhang, X., et al.: Moa-vr: A mixture-of-agents system towards all-in-one video restoration. IEEE Journal of Selected Topics in Signal Processing (2025)
- [30] Liu, S., Han, Y., Xing, P., Yin, F., Wang, R., Cheng, W., et al.: Step1x-edit: A practical framework for general image editing. arXiv preprint arXiv:2504.17761 (2025)
- [31] Lou, J., Ma, L., Hu, K.X., Yang, H., Lin, W.Y.: Transalnet: Towards perceptually relevant visual saliency prediction. Neurocomputing **507**, 250–264 (2022)
- [32] Lu, S., Li, Y., Xia, Y., Hu, Y., Zhao, S., Ma, Y., et al.: Ovis2.5 technical report. arXiv:2508.11737 (2025)
- [33] Luo, X., Wang, J., Wu, C., Xiao, S., Jiang, X., Lian, D., et al.: Editscore: Unlocking online rl for image editing via high-fidelity reward modeling. arXiv preprint arXiv:2509.23909 (2025)
- [34] Lupascu, M., Stupariu, M.S.: Optimal transport for rectified flow image editing: Unifying inversion-based and direct methods. arXiv preprint arXiv:2508.02363 (2025)

- [35] Mao, C., Zhang, J., Pan, Y., Jiang, Z., Han, Z., Liu, Y., Zhou, J.: Ace++: Instruction-based image creation and editing via context-aware content filling. arXiv preprint arXiv:2501.02487 (2025)
- [36] Mikolov, T., Chen, K., Corrado, G., Dean, J.: Efficient estimation of word representations in vector space. arXiv preprint arXiv:1301.3781 (2013)
- [37] Nam, H., Kwon, G., Park, G.Y., Ye, J.C.: Contrastive denoising score for text-guided latent diffusion image editing. In: Proceedings of the IEEE/CVF Conference on Computer Vision and Pattern Recognition (CVPR). pp. 9192–9201 (June 2024)
- [38] OpenAI: Chatgpt 5. <https://openai.com/gpt-5/> (2025)
- [39] OpenAI: Gpt-5. <https://www.openai.com> (2025)
- [40] Qian, Y., Bocek-Rivele, E., Song, L., Tong, J., Yang, Y., Lu, J., et al.: Pico-banana-400k: A large-scale dataset for text-guided image editing. arXiv preprint arXiv:2510.19808 (2025)
- [41] Rombach, R., Blattmann, A., Lorenz, D., Esser, P., Ommer, B.: High-resolution image synthesis with latent diffusion models. In: Proceedings of the IEEE/CVF Conference on Computer Vision and Pattern Recognition (CVPR). pp. 10684–10695 (2022)
- [42] Seedream, T., Chen, Y., Gao, Y., Gong, L., Guo, M., Guo, Q., et al.: Seedream 4.0: Toward next-generation multimodal image generation. arXiv preprint (2025)
- [43] Sheikh, H.R., Bovik, A.C.: Image information and visual quality. *IEEE Transactions on Image Processing (TIP)* **15**(2), 430–444 (2006)
- [44] Shen, S., Liang, J., Cai, C., Geng, C., Duan, H., Zhang, X., et al.: Agentic retoucher for text-to-image generation. In: Proceedings of the IEEE/CVF Conference on Computer Vision and Pattern Recognition (CVPR) (2026)
- [45] Wang, J., Duan, H., Zhai, G., Min, X.: Quality assessment for ai generated images with instruction tuning. *IEEE Transactions on Multimedia (TMM)* (2026)
- [46] Wang, J., Duan, H., Zhao, Y., Wang, J., Zhai, G., Min, X.: Lmm4lmm: Benchmarking and evaluating large-multimodal image generation with lmm. In: Proceedings of the IEEE/CVF International Conference on Computer Vision (ICCV). pp. 17312–17323 (2025)
- [47] Wang, J., Wang, J., Duan, H., Kang, J., Zhai, G., Min, X.: I2i-bench: A comprehensive benchmark suite for image-to-image editing models. arXiv preprint arXiv:2512.04660 (2025)
- [48] Wang, L., Xing, X., Cheng, Y., Zhao, Z., Donghao, L., Tiankai, H., et al.: Promptenhancer: A simple approach to enhance text-to-image models via chain-of-thought prompt rewriting. arXiv preprint arXiv:2509.04545 (2025)
- [49] Wang, W., Gao, Z., Gu, L., Pu, H., Cui, L., Wei, X., et al.: Internvl3.5: Advancing open-source multimodal models in versatility, reasoning, and efficiency. arXiv preprint arXiv:2508.18265 (2025)
- [50] Wang, Z., Bovik, A.C., Sheikh, H.R., Simoncelli, E.P.: Image quality assessment: from error visibility to structural similarity. *IEEE Transactions on Image Processing (TIP)* **13**(4), 600–612 (2004)
- [51] Wei, H., Liu, H., Wang, Z., Peng, Y., Xu, B., Wu, S., et al.: Skywork unipic 3.0: Unified multi-image composition via sequence modeling. arXiv preprint arXiv:2601.15664 (2026)
- [52] Wu, C., Li, J., Zhou, J., Lin, J., Gao, K., Yan, K., et al.: Qwen-image technical report. arXiv preprint arXiv:2508.02324 (2025)
- [53] Wu, C., Zheng, P., Yan, R., Xiao, S., Luo, X., Wang, Y., et al.: Omnigen2: Exploration to advanced multimodal generation. arXiv preprint arXiv:2506.18871 (2025)
- [54] Wu, H., Zhang, Z., Zhang, W., Chen, C., Li, C., Liao, L., et al.: Q-align: Teaching lmm for visual scoring via discrete text-defined levels. arXiv preprint arXiv:2312.17090 (2023)

- [55] Wu, K., Jiang, S., Ku, M., Nie, P., Liu, M., Chen, W.: Editreward: A human-aligned reward model for instruction-guided image editing. arXiv preprint arXiv:2509.26346 (2025)
- [56] Wu, Q., Bansal, G., Zhang, J., Wu, Y., Li, B., Zhu, E., et al.: Autogen: Enabling next-gen llm applications via multi-agent conversation. arXiv preprint arXiv:2308.08155 (2023)
- [57] Wu, Y., Li, Z., Hu, X., Ye, X., Zeng, X., Yu, G., Zhu, W., Schiele, B., Yang, M.H., Yang, X.: Kris-bench: Benchmarking next-level intelligent image editing models. arXiv preprint arXiv:2505.16707 (2025)
- [58] Wu, Y., Li, Z., Hu, X., Ye, X., Zeng, X., Yu, G., et al.: Kris-bench: Benchmarking next-level intelligent image editing models. arXiv preprint arXiv:2505.16707 (2025)
- [59] Xia, B., Peng, B., Zhang, Y., Huang, J., Liu, J., Li, J., et al.: Dreamomni2: Multimodal instruction-based editing and generation. arXiv preprint arXiv:2510.06679 (2025)
- [60] Xu, Z., Duan, H., Ji, Z., Zhang, X., Liu, Y., Min, X., et al.: Edithf-1m: A million-scale rich human preference feedback for image editing. arXiv preprint arXiv:2603.14916 (2026)
- [61] Xu, Z., Duan, H., Liu, B., Ma, G., Wang, J., Yang, L., et al.: Lmm4edit: Benchmarking and evaluating multimodal image editing with lmm. In: Proceedings of the ACM International Conference on Multimedia (ACM MM). pp. 6908–6917 (October 2025)
- [62] Xu, Z., Duan, H., Ma, G., Yang, L., Wang, J., Wu, Q., et al.: Harmonyiq: Pioneering benchmark and model for image harmonization quality assessment. In: IEEE International Conference on Multimedia and Expo (ICME). pp. 1–6 (2025)
- [63] Xu, Z., Shen, D., Du, Y., Hao, K., Huang, J., Huang, X.: Magicwand: A universal agent for generation and evaluation aligned with user preference (2025)
- [64] Xue, W., Zhang, L., Mou, X., Bovik, A.C.: Gradient magnitude similarity deviation: A highly efficient perceptual image quality index. IEEE Transactions on Image Processing (TIP) **23**(2), 684–695 (2013)
- [65] Yang, A., Li, A., Yang, B., Zhang, B., Hui, B., Zheng, B., et al.: Qwen3 technical report. arXiv preprint arXiv:2505.09388 (2025)
- [66] Yang, L., Duan, H., Wang, J., Liu, J., Hu, M., Min, X., Zhai, G., Le Callet, P.: Quality assessment and distortion-aware saliency prediction for ai-generated omnidirectional images. IEEE Transactions on Circuits and Systems for Video Technology (2025)
- [67] Ye, R., Zhang, J., Liu, Z., Zhu, Z., Yang, S., Li, L., et al.: Agent banana: High-fidelity image editing with agentic thinking and tooling. arXiv preprint arXiv:2602.09084 (2026)
- [68] Yin, G., Wang, W., Yuan, Z., Han, C., Ji, W., Sun, S., et al.: Content-variant reference image quality assessment via knowledge distillation. In: Proceedings of the Conference on Association for the Advancement of Artificial Intelligence (AAAI). vol. 36, pp. 3134–3142 (2022)
- [69] Zhang, K., Mo, L., Chen, W., Sun, H., Su, Y.: Magicbrush: A manually annotated dataset for instruction-guided image editing. In: Proceedings of the Advances in Neural Information Processing Systems (NeurIPS) (2023)
- [70] Zhang, R., Isola, P., Efros, A.A., Shechtman, E., Wang, O.: The unreasonable effectiveness of deep features as a perceptual metric. In: Proceedings of the IEEE/CVF Conference on Computer Vision and Pattern Recognition (CVPR) (2018)
- [71] Zhao, Q., Cai, J.: Visual saliency detection by spatially weighted dissimilarity. In: 2011 IEEE CVPR. pp. 1241–1248. IEEE (2011)
- [72] Zhu, K., Gu, J., You, Z., Qiao, Y., Dong, C.: An intelligent agentic system for complex image restoration problems. arXiv preprint arXiv:2410.17809 (2024)